JOURNAL OF SPACECRAFT AND ROCKETS
Vol. 44, No. 5, September–October 2007

Noise Transmission Studies of an Advanced Grid-Stiffened Composite Fairing

Steven A. Lane*
U.S. Air Force Research Laboratory, Kirtland AFB, New Mexico 87117
Scott Kennedy†
CSA Engineering, Albuquerque, New Mexico 87123
and
Robert Richard‡
Boeing-SVS, Albuquerque, New Mexico 87109

DOI: 10.2514/1.28590

Interior fairing noise is an important consideration for payload launch survivability and has been studied extensively since the beginning of the space program. This work presents acoustic transmission studies conducted by the Air Force Research Laboratory, Space Vehicles Directorate, on a composite, grid-stiffened, Minotaur payload fairing. These tests were performed in an acoustics laboratory and examined the effects of acoustic flanking paths, the thermal protection system, and melamine-type acoustic blanket treatments on fairing noise. The data showed that acoustic flanking paths significantly increase noise transmission, especially at low frequency. The bare fairing with thermal protection system provided approximately 14 dB of noise reduction over the 5000 Hz bandwidth relative to external levels. Acoustic blanket performance was measured as a function of bandwidth, surface area coverage, and mass. It was observed that small amounts of treatment (2 kg) significantly increased noise reduction (3.6 dB), even at low frequency.

I. Introduction

ACOUSTIC levels generated by large launch vehicles can pose significant risk for payload launch survivability. The interior vibroacoustic launch environment in the next generation of composite fairings being developed by the U.S. Air Force may potentially be more severe because the fairings will be less massive and have less structural damping, both factors that contribute to increased noise transmission [1]. Acoustic loads generated during the first few seconds of launch tend to be the worst, but there are other events that generate significant internal acoustic loads, such as maximum dynamic pressure and transonic crossover [2,3]. Launch vehicle acoustics have been studied since the beginning of the space program. A NASA publication on launch acoustics published in 1971 presents a good discussion and a list of references for work performed up to that time [4]. Publications by McInerny et al. [5,6] provide very good discussions and additional references on more recent research regarding launch acoustics.

Acoustic blankets play an important role in reducing the fairing acoustic environment during the ascent into orbit. Research has been conducted to study and improve acoustic blanket designs for launch vehicles, but it is always a trade between acoustic reduction, blanket mass, and volume. In the late 1990s, the expected acoustic loads in the Titan launch vehicle used to launch the Cassini spacecraft exceeded the acceptable levels; thus improved acoustic blankets were designed specifically for that mission. The improved blanket used layers of different materials and was successful, but required a significant increase in blanket thickness and weight [7].

The evolved expendable launch vehicle (EELV) programs have conducted research to ensure that their launch vehicles meet military specifications as defined by the Standard Interface Specification [8]. The Atlas V launch vehicle, produced by Lockheed–Martin, uses an aluminum fairing that is 4 to 5 m in diameter. The Atlas V 500 and heavy lift vehicles use a fairing designed and built by Contraves, which builds the Ariane V launch vehicle for the European Space Agency. Contraves developed an innovative acoustic blanket for fairing noise reduction that uses tunable acoustic absorbers integrated into foam and plastic mats. The foam and plastic mats provide broadband noise absorption, and the acoustic absorbers are tuned for a particular frequency range of interest [9]. The Atlas V also incorporates a water suppression system to reduce the external acoustic loads generated by the engines at launch [10]. The Delta-IV, developed by Boeing, uses a silicon-bonded, heat-treated, glass-fiber batting as its standard acoustic blanket [11].

The U.S. Air Force Research Laboratory, U.S. Air Force Office of Scientific Research, Orbital Sciences Corporation, and Boeing have jointly developed an advanced, grid-stiffened, composite fairing designed for the Minotaur launch vehicle [12]. This fairing was made using a graphite-epoxy composite and measures about 5 m in length. Acoustic transmission studies were conducted to assess 1) the impact of acoustic flanking paths, 2) the performance of acoustic blanket materials as measured by a noise reduction metric, and 3) the impact of the thermal protection system (TPS) on noise transmission. At launch, external loads on a Minotaur are approximately 145 dB, depending on the stack and launch pad. This paper will present some background on fairing structural-acoustic transmission, discuss the test loads used in this work, and discuss the acoustic blankets that were tested. Experimental data demonstrating the performance of the acoustic blanket material at high sound pressure levels will be given to justify extrapolation of the results from laboratory sound pressure levels to launch levels. Finally, analysis of the test data and conclusions regarding the design of acoustic treatments for fairings to meet volume or mass constraints are given.

II. Theory

A. Modeling

Modeling the noise transmission through a grid-stiffened, composite fairing is difficult due to the following issues: 1) the complexity of modeling the ribs and composite shells, 2) the

Received 27 October 2006; revision received 8 November 2006; accepted for publication 1 December 2006.

*Senior Research Aerospace Engineer, AFRL/VSE, 3550 Aberdeen Avenue SE; steven.lane@kirtland.af.mil. Senior Member AIAA.
†Mechanical Engineer, 1300 Britt Street. Member AIAA.
‡Senior Mechanical Engineer, 4411 The 25 Way. Member AIAA.

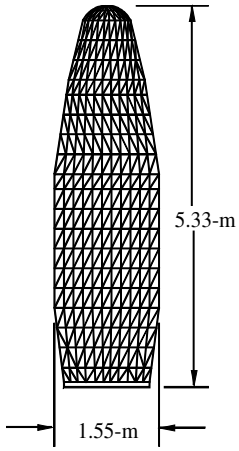

Fig. 1 Fairing geometry used in modeling and numerical simulations.

difficulty in accurately describing the boundary conditions, 3) the inability to adequately model structural-acoustic coupling and damping, 4) the complexity of modeling the external sound field, 5) the difficulty in accurately accounting for ports, hatches, seams, and pad-ups (reinforcement layers), and 6) the uncertainty introduced by the nonuniform behavior of the structure. To predict noise transmission, structural-acoustic models must cover a wide bandwidth, starting around 30–40 Hz and extending to 6000–10,000 Hz. Vipperman et al. [13] studied noise transmission through a small grid-stiffened composite cylinder. They developed and validated numerical models and identified important parameters for characterizing sound transmission.

In 1999, Griffin et al. [14] developed fully coupled, structural-acoustic models of a composite Minotaur fairing based on the then current conceptual design of the fairing presented later. The model was developed for the purpose of low frequency noise transmission analysis and for evaluating active noise control methods. The geometry used for their model is presented in Fig. 1. The coupled model was developed by coupling the in vacuo structural model with a rigid-wall acoustic model using a modal-interaction approach [15]. The material properties for the fairing model were determined by assuming homogeneous shell elements and composite stiffness matrices. The ribs and face sheets were not modeled individually; instead, smeared properties were estimated and used in the model. The mode shapes for the uncoupled subsystems were computed using NASTRAN, assuming 50 structural modes and 50 acoustic modes. It was verified that the use of 100 modes sufficiently converged the model for a bandwidth up to 300 Hz. A damping ratio of 1.5% was assumed for both the structural modes and the acoustic modes. The total weight of the modeled fairing was 63.6 kg (140 lb). Several of the frequency response functions from structural nodes (input) to internal acoustic volume nodes (outputs) are given in Fig. 2.

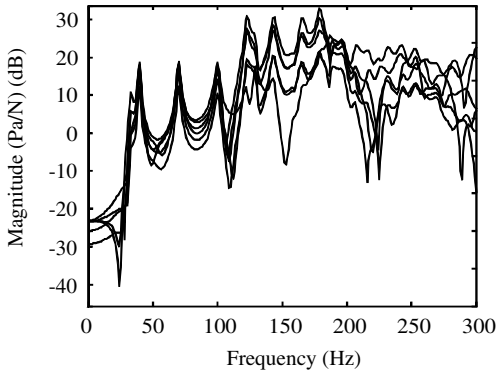

Fig. 2 Representative transfer functions from the coupled model developed by Griffin et al.

There were several relevant observations to be noted from the work on the coupled model developed by Griffin. First, the low frequency response was dominated by the acoustic resonances. These are observable in Fig. 2 at about 35, 70, and 100 Hz. Second, the addition of structural mass or structural damping did not have a significant effect on the interior acoustic response. Damping of the acoustic resonances was determined to be the most effective method to reduce the interior response. Third, it was observed that at frequencies where both structural and acoustic modes were proximal, there was increased response as a consequence of more efficient coupling between the structural and acoustic modes. The fairing structure acted like a filter between the external disturbance and the internal volume, with a structural-acoustic feedback loop occurring between the structural and acoustic modes.

The models developed by Griffin et al. did not include descriptions of separation seams, ports, hatches, or the TPS—features that exist on real fairings but were not adequately defined at the time of their work. Separation seams introduce discontinuities and structural ribs create localized stiffening, both of which impact structural-acoustic transmission. Openings in the fairing (including ports, gaps, and hatches) create potential acoustic flanking paths, which can be thought of as acoustic short circuits. The effect of these will be shown in the subsequent test results. The TPS, which protects the fairing during ascent, is made largely from a cork-type mixture that is applied over the entire fairing exterior, and significantly impacts the acoustic transmission through the fairing. Consequently, numerical models, such as the aforementioned finite element model, do not yield accurate predictions of the transmission of the as-built fairing. In fact, finite element models are typically only used for coupled loads analysis, and statistical energy analysis (SEA) is used for vibroacoustic modeling and analysis [16,17]. SEA models provide a transmission estimate that is averaged with respect to both frequency and space (physical dimensions). Such models do not include very much detail and can have significant error at low frequency where modal density is low. Therefore, it is pertinent to understand the effects of seams, openings, TPS, and blanket treatments when developing vibroacoustic models and interpreting simulation results.

B. Disturbance Loading

A critical issue for evaluating the performance of acoustic treatments in fairings is determining an appropriate external loading condition for the testing. Naturally, realism is desired, but unless one is willing to set up the test near a pending launch, a compromise in realism must be made. Generally, fairings are qualification tested in very large reverberation chambers capable of generating 150+ dB disturbance loads (the same chambers used for qualification testing of payloads). However, reverberation chambers are not representative of actual launch loads acting on a fairing because the disturbance field is spatially correlated over the surface. In reality, the fairing is usually many meters above the ground, away from the rocket engines and thrust tunnels. The sound impinges on the fairing from direct radiation and ground reflections that arrive as plane waves traveling at oblique angles. This loading condition would be very different than a reverberant acoustic field, which is spatially coherent, or a diffuse field, which is completely incoherent.

As a compromise between a reverberant field and a completely diffuse field, the tests presented here were conducted in large, semireverberant laboratories using an array of speaker equipment to tailor the external disturbance over three test bandwidths: 40–500 Hz, 40–2000 Hz, and 40–5000 Hz (40 Hz was the approximate roll-off frequency of our subwoofers). The laboratories were constructed from concrete and cinder block walls and included many scattering surfaces that produced an approximately diffuse disturbance loading on the fairing. This approach was chosen because a laboratory environment was more controllable and the experiments were more repeatable (thus reducing measurement uncertainty) than if they had been conducted outdoors. Although an outdoor test would arguably be more realistic, repeatability was a concern. Because a primary objective of this program was to study

the noise reduction provided by various acoustic blanket treatments, a consistent disturbance loading was needed.

C. Procedure for Computing Noise Reduction

Noise transmission and acoustic blanket performance were measured by computing the noise reduction, which is defined here to be the ratio of the spatially averaged external sound field impinging on the fairing to the spatially averaged interior acoustic response. Acoustic transmission through flat panels is typically measured using transmission loss, but this quantity is not reasonable for a closed cylinder [18]. Noise reduction was computed over each bandwidth (i.e., 40–500 Hz, 40–2000 Hz, 40–5000 Hz) using the expression:

$$\mathrm{NR\,(dB)} = 20\log_{10}\left(\frac{\text{External rms}}{\text{Internal rms}}\right) \tag{1}$$

This is similar to the noise reduction metric given by Hansen [19]. To estimate the "External rms" (where rms denotes root-mean square) of the external sound field, microphone measurements were taken at many locations around the fairing exterior and spatially averaged. The "Internal rms" was estimated in a similar way by taking microphone measurements at many locations throughout the fairing interior.

D. Acoustic Blanket Tests

There is no standard acoustic blanket for payload fairings. Treatments vary from manufacturer to manufacturer and are often tailored for particular fairings and/or payloads. Acoustic blankets can be fabricated like quilts, consisting of many layers of sound absorbing fiber material, or consist of foam-type material. Different blanket designs can be used to target different frequency bands, and acoustic treatments can combine transmission loss with acoustic absorption. Fairing blankets must be designed and packaged to meet outgassing specifications and/or cleanliness standards. A secure attachment is necessary to prevent the blanket from detaching during launch and striking the payload or interfering with deployment. Different blanket systems require different attachment methods.

Melamine acoustic foam was chosen as the representative acoustic blanket material for this work. It has a low density ($\sim$8.9 kg/m^3) and low outgassing. The absorption curve for 5-cm foam as given by the manufacturer is shown in Fig. 3 (measured per ASTM C423-90A). As typical for acoustic foam, its absorption rolls off at low frequency. This is why large amounts are required to attenuate low frequency disturbances.

Concern was raised early in the program regarding the behavior of the material at high sound pressure levels. The question was whether noise reduction measurements made at 90–100 dB were reliable indicators of performance at higher sound pressure levels (130–140 dB). Therefore, a series of tests were conducted in a test cylinder using a high-output actuator to determine if the noise reduction provided by two foam samples (2.5 and 5 cm) was linear with respect to sound pressure level. Data from those tests are presented in Fig. 4. The data show some scatter (standard deviation less than 0.23 dB),

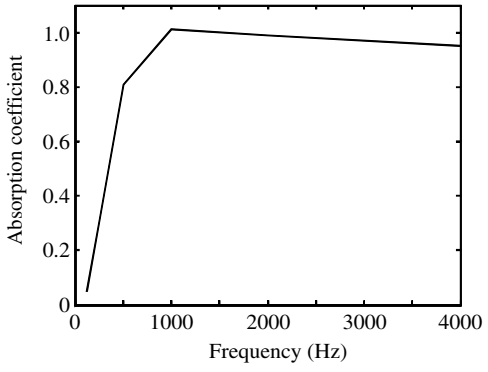

Fig. 3 Manufacturer absorption curve for 5-cm melamine foam.

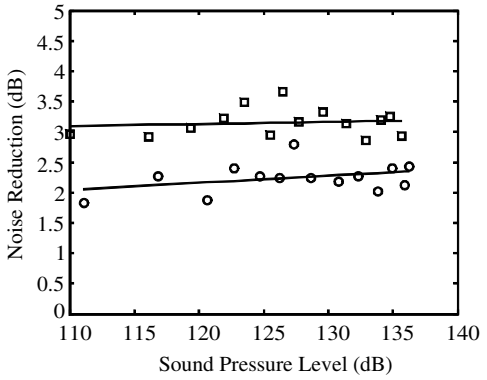

Fig. 4 Noise reduction as a function of sound pressure level: ○, 2.5-cm foam; □, 5-cm foam.

but linear regressions of the measured data indicate that the trend provided by the foam was in fact reasonably constant with respect to sound pressure level, at least up to 136 dB (relative to 20 μPa). Therefore, if laboratory tests on the fairing showed 20 dB of reduction at 100 dB, we are reasonably confident that we would see the same 20 dB of reduction at 140 dB (assuming consistent spectral content).

III. Experimental Setup

The fairing used for this work was fabricated by Boeing using two half-shells connected by rails that ran along the axial length of the fairing. Figure 5 shows one of the composite half-shells (interior view). Figure 6 shows some of the utility ports of the lower fairing section. The mass of the actual qualification test fairing fabricated by

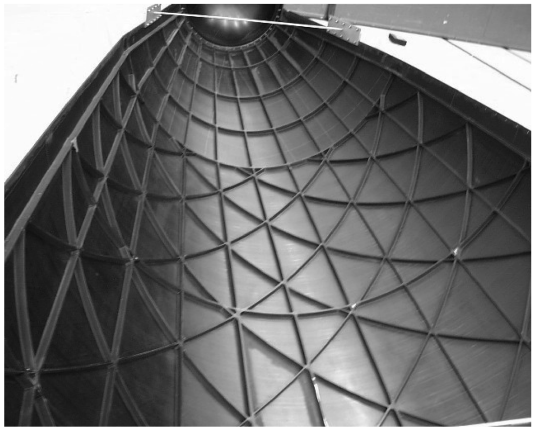

Fig. 5 Interior view of the Minotaur fairing half-shell.

Fig. 6 Illustration of utility ports in the Minotaur fairing.

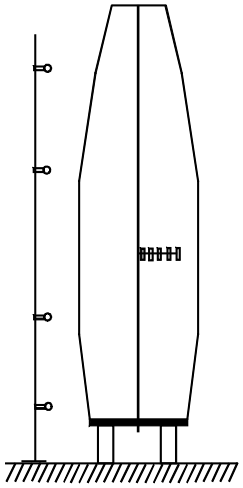

Fig. 7 Illustration of internal and external microphone booms.

Boeing was approximately 118 kg (260 lb), not counting the thermal protection system, which was approximately 16 kg (the TPS layer was roughly 6 mm thick). The as-built mass was greater than the modeled mass (63.6 kg) because additional composite layers were used to reinforce the area around the ports and hatches.

Figure 7 shows schematically the microphone booms used for data measurement in the experiments. The external acoustic field was measured using four microphones (PCB Model 130C10, sensitivity = 21.6 mV/Pa, dynamic range = 20–7000 Hz ± 1 dB, linearity ⟨3%⟩ 128 dB sound pressure level) at various positions along the axial length of the fairing and at various positions around the fairing circumference. The internal response was measured using a microphone boom with five attached microphones. The internal microphone boom was connected to a cable-and-pulley apparatus inside the fairing that permitted the boom to be maneuvered inside the closed fairing. The microphone boom extended radially from the fairing centerline. Measurements were made at several positions along the length of the fairing and at different rotation angles to adequately sample the internal response. The microphone signals were high-pass filtered (fourth order Butterworth, cutoff frequency of 20 Hz) in MATLAB [20] to remove any dc coupling. The rms values of the microphone signals were averaged to yield an overall spatial average. Sound pressure levels were computed relative to a reference pressure of 20 μPa.

Initial tests were performed on the bare fairing by measuring the external response at 96 microphone positions, and the internal response at 195 microphone positions. Using such a large number of measurements ensured convergence of the spatial averaging approach to the "true" rms values. Subsequently, the number of measurements was reduced to a subset of measurements that adequately represented the true spatial averages. It was determined that 48 external measurements and 65 internal measurements were sufficient to describe the spatial averages without introducing experimental uncertainty greater than ±0.2 dB over each bandwidth, based on observations of test-to-test repeatability.

Tests were then conducted on the bare fairing (no thermal protection system) and characterized bare fairing noise reduction, the effect of openings (open hatches, unplugged gaps in the separation rails, and open ports), and the performance of 5-cm melamine foam. The final tests were conducted on the fairing with the thermal protection system and compared the noise reduction provided by 2.5, 5, and 10-cm melamine foam blanket treatments. In both cases, the foam was cut into narrow strips to fit into the fairing interior and the strips were attached to the ribs using Velcro. The Velcro had sufficient flexibility between the top and bottom adhesive layers to allow the melamine to relax to a stress-free position. Because the density of the melamine was so low, only a very small amount of Velcro was required to hold a large foam strip in place. In both test cases, an overhead crane was attached to the fairing's nose and used to lift it to a vertical position. The fairing then rested on blocks that supported the fairing approximately 40 cm off of the floor. Tests were conducted in similar labs, but due to scheduling of other experiments, the same laboratory could not be used for both sets of tests.

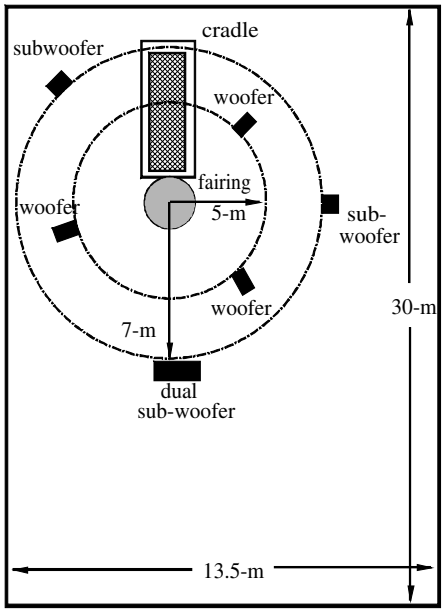

Fig. 8 Laboratory setup for the first set of fairing measurements.

A. Fairing with No Thermal Protection System

The laboratory layout used for the first set of tests is given in Fig. 8. Two subwoofers mounted individually in sealed cabinets and one dual subwoofer system were used to generate low frequency (40–500 Hz) excitation. Three woofer cabinets, each consisting of four woofers, were used to generate the disturbance from approximately 500 to 5000 Hz, although there was considerable roll-off above 2500 Hz.

Figure 9 shows the bare fairing in the vertical test position. The graphite-epoxy composite had a dull, black finish. The aluminum

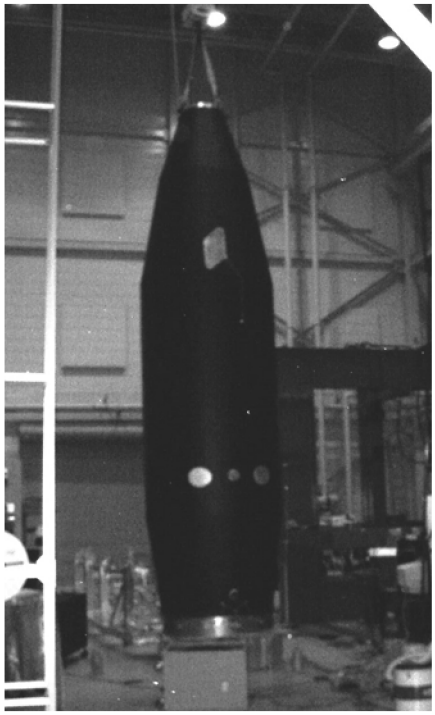

Fig. 9 Minotaur fairing without TPS.

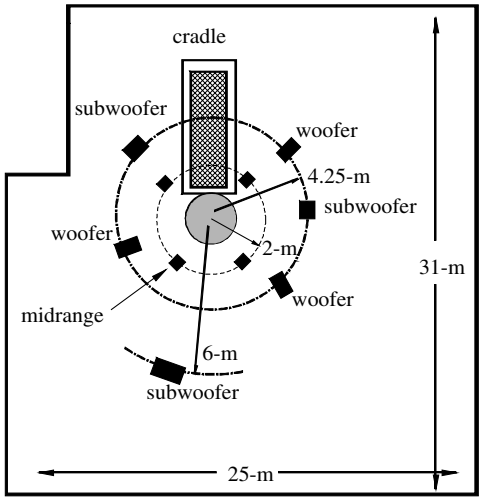

Fig. 10 Laboratory setup for the second set of fairing measurements.

hatch and port covers can clearly be seen in this picture. The covers were about 3 mm thick and were curved to match the curvature of the outer fairing shell. The covers were attached to the fairing using a commercial elastic adhesive/sealant material. The nose of the fairing was bolted to a thick aluminum end cap that had straps to which the crane was attached. The bottom (aft) end cap was fabricated using two medium density particleboard layers that were separated by foam rubber insulation. The base of the fairing was bolted to an aluminum-mounting ring that was connected by a hinged platform to the fairing's cradle. The hinged platform allowed the fairing to be pivoted from horizontal to vertical positions.

B. Fairing with Thermal Protection System

The laboratory layout used for the second set of tests is given in Fig. 10. The audio system was augmented with four midrange speakers, each individually mounted in sealed cabinets, to boost the 1500–5000 Hz bandwidth. A crossover and an equalizer were included to provide a more spectrally flat disturbance field. Figure 11 compares the spatially averaged external sound pressure levels computed over 1/3-octave bands with and without the additional midrange speakers and audio equipment. This was done to improve the signal-to-noise ratio of the internal measurements, particularly above 2000 Hz. The data presented in Fig. 11 do not represent the same overall sound pressure levels, but do demonstrate that less amplitude variation was achieved over the bandwidth. More important, the roll-off above 2 kHz was eliminated.

Figure 12 shows the fairing in the vertical test position. The thermal protection system was painted white and covered most of the fairing's exterior. Laser reflector patches can be seen along the (vertical) separation rail, which were applied and used during prior

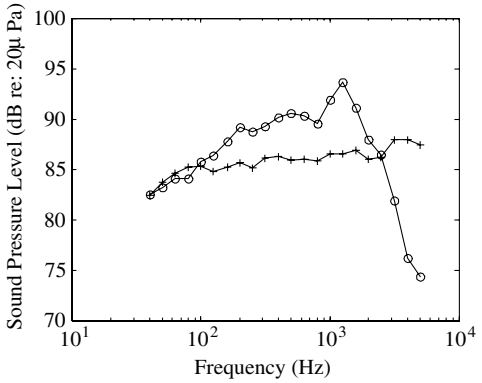

Fig. 11 Spatially averaged (third octave) external sound pressure levels: ○, spectrum analyzer, power amps, subwoofers, and woofers; +, with additional crossover, equalizer, and midrange speakers.

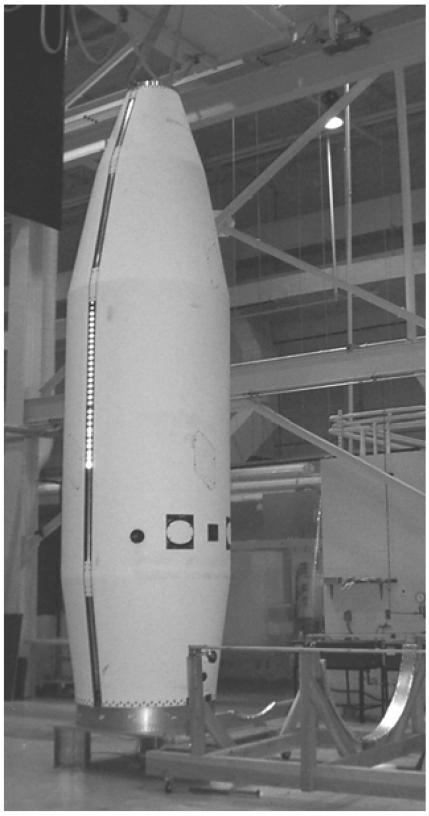

Fig. 12 Minotaur fairing with TPS.

mechanical testing. The cradle can be seen to the right of the fairing. At the base of the fairing, one can see the blocks supporting the aft end above the ground (∼40 cm).

IV. Results

A. Fairing with No Thermal Protection System

The noise reduction of the bare fairing (no TPS or acoustic blankets) for various amounts of removed surface area was measured and is presented in Fig. 13. In these tests, hatch covers, port covers, and gap plugs were incrementally removed from the fairing to create acoustic flanking paths. The change in noise reduction is plotted as a function of the percentage of the total fairing surface area removed. The data show that the noise reduction provided by the fairing with no openings was about 7.2, 6.7, and 6.6 dB across the 500, 2000, and 5000 Hz bandwidths, respectively. The noise reduction did not change very much over the three bandwidths until about 0.1% of the surface area was removed. Then, the low frequency noise reduction shows the most significant change. At 1.2%, the noise reduction was reduced to about 4.3, 5.0, and 5.1 dB across the 500, 2000, and

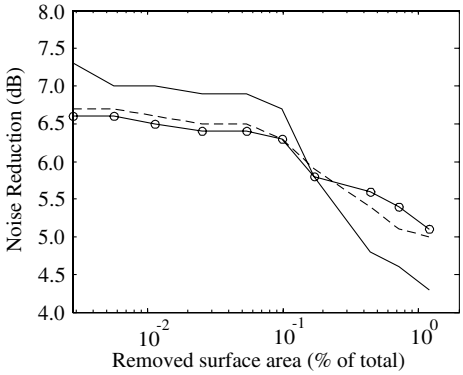

Fig. 13 Noise reduction of the bare fairing with holes/openings (no foam treatment): solid line, 500 Hz; dashed line, 2000 Hz; ○, 5000 Hz.

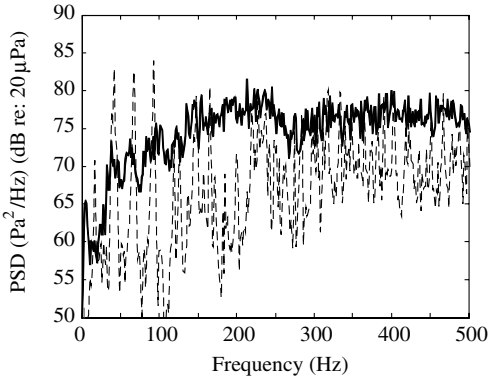

Fig. 14 Response of the bare fairing with 1.2% holes/openings (no foam treatment): solid line, external; dashed line, internal.

5000 Hz bandwidths, respectively. In each case, removing hatches, port covers, and plugs increased the noise transmission, and the effect did not appear to be a linear function of removed surface area. External levels used for these tests were approximately 104.0 ± 0.5 dB for the 500 Hz bandwidth, 102.7 ± 0.2 dB for the 2000 Hz bandwidth, and 98.8 ± 0.2 dB for the 5000 Hz bandwidth. For each test, the data were measured multiple times and averaged to reduce measurement uncertainty. The measurement uncertainty for these tests was estimated to be less than ±0.1 dB based on test-to-test repeatability observations.

Figure 14 presents the power spectral density (PSD) of the spatially averaged interior response superimposed on the PSD of the averaged external response for the case of 1.2% open surface area over the 500 Hz bandwidth. Notice how the interior response equals or exceeds the amplitude of the exterior response across the bandwidth (e.g., 150, 165, 310, 330, 470 Hz), and particularly at the first three acoustic resonances (36, 67, and 90 Hz). In fact, the interior acoustic response at these frequencies was nearly an order of magnitude (10 dB) greater than the external disturbance levels. This agrees with the prior observation in Fig. 13 that the low frequency response was more significantly affected than the higher frequency response. Also note the internal resonance peak occurring at approximately 20 Hz. This is not a standing wave within the fairing volume, but rather a "breathing mode" or "Helmholtz mode" that results from having openings in the fairing. The sum of the air mass at the openings (i.e., where the panels were removed) acts as a lumped mass oscillating on an air spring provided by the fairing volume, like a large Helmholtz resonator.

In Fig. 14, the fluctuations of the internal and external spectra as a function of frequency are given, and from this, one can observe the influence of specific resonances on the overall response. However, as the bandwidth increases, and multiple plots are superimposed, it becomes difficult to analyze and interpret the data. Therefore,

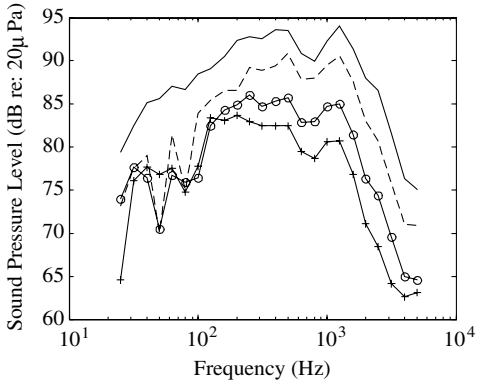

Fig. 15 Spatially averaged third octave band sound pressure levels, no TPS, 5-cm acoustic foam treatment: solid line, external; dashed line, no foam; ○, 50% coverage; +, 93% coverage.

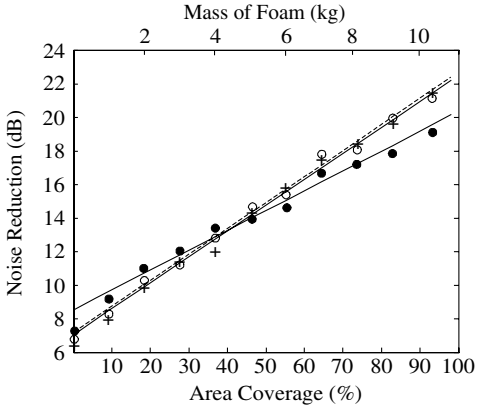

Fig. 16 Noise reduction using 5-cm acoustic foam treatment, no TPS: ●, 500 Hz; ○, 2000 Hz; +, 5000 Hz.

subsequent plots will present data that have been averaged over one-third octave bandwidth as defined by Hansen [21].

Next, 5-cm melamine foam was attached to the fairing interior using a small amount of Velcro. All hatch covers and port covers were reattached to the fairing, and all other gaps were plugged with high-density rubber. The foam was first added to the ends of the fairing, where the amplitudes of the acoustic modes were largest. Then, additional foam was added incrementally, moving from the ends toward the middle of the fairing. Area coverage was estimated from the ratio of the internal surface area of the fairing to the area of the foam added. Because the foam did not form fit the fairing interior, and gaps were sometimes unavoidable, 100% coverage was not attainable.

Figure 15 presents the exterior and interior sound pressure levels averaged over one-third octave bandwidths for the case of no foam, 50% surface area coverage, and 93% interior surface area coverage. This figure shows the effect of the added foam as a function of frequency. In this test case, all interior levels were less than exterior levels. Below 200 Hz, the interior responses were similar, indicating that the acoustic foam had little effect on the band averages at low frequency. Separation between the curves was somewhat constant above 400 Hz (about 5 dB), indicating that foam performance (i.e., noise reduction) was less a function of frequency above 400 Hz, and more a function of the amount added.

In Fig. 16, the noise reduction is presented for each of the three test bandwidths (40–500 Hz, 40–2000 Hz, 40–5000 Hz), and is presented as both a function of surface area coverage and as a function of blanket mass. For each bandwidth, linear regressions were computed for the corresponding data and are superimposed on the data points. In each case, there were similar trends and the noise reduction appears to be somewhat linear with respect to the amount of acoustic treatment. Figure 16 shows that the bare fairing noise reduction was between 6.0 and 7.5 dB, which agrees with Fig. 13. The noise reduction across the 2000 and 5000 Hz bandwidths increased at about the same rate. At nearly 93% coverage, which corresponded to about 11 kg (24 lb) of foam, the noise reduction across the 5000 Hz bandwidth was about 22.0 dB. External disturbance levels were similar to those used for Fig. 13, and the spectra consistent with that shown in Fig. 15. The combined experimental uncertainty and measurement uncertainty for this data was determined to be less than ±0.2 dB based on test-to-test repeatability.

B. Fairing with Thermal Protection System

Next, performance measurements from three different thicknesses of acoustic foam material taken using the fairing with TPS are presented. As with the previous set of tests, performance will be given as a function of frequency, and as a function of mass and surface area coverage. The fairing was in the vertical position for all tests, all hatch and port covers attached, and all gaps plugged.

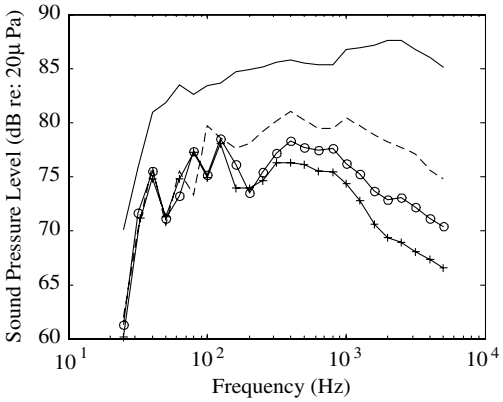

Fig. 17 Spatially averaged sound pressure levels in third octave bandwidths for 2.5-cm acoustic foam treatment: solid line, external; dashed line, no foam; ○, 50% coverage; +, 90% coverage.

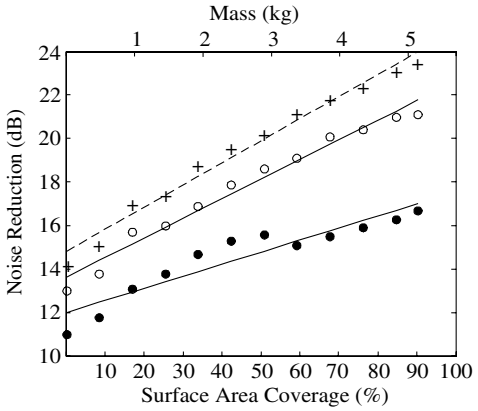

Fig. 18 Noise reduction using 2.5-cm acoustic foam treatment, with TPS, as a function of area coverage and mass: ●, 500 Hz; ○, 2000 Hz; +, 5000 Hz.

Figure 17 shows the external and internal spatially averaged 1/3-octave band levels as a function of frequency for the 2.5-cm foam tests over the 5000 Hz bandwidth. The overall external disturbance level was computed to be about 98.9 dB (re: 20 μPa). There was more separation between the external levels and the internal (no foam) levels than in Fig. 15, attributable to the TPS. The acoustic foam provided little effect below 200 Hz.

Figure 18 summarizes the average measured noise reductions for the 2.5-cm treatment as a function of surface area and mass for all three bandwidths. The external sound levels were approximately 110 dB (500 Hz), 107 dB (2000 Hz), and 99 dB (5000 Hz). Linear regressions are superimposed. The noise reduction for no treatment was about 11 dB (500 Hz), 13 dB (2000 Hz), and 14 dB (5000 Hz).

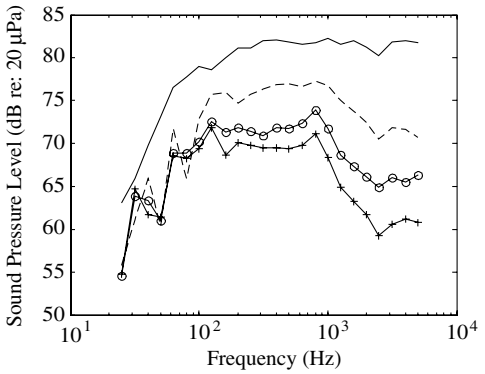

Fig. 19 Spatially averaged sound pressure levels in third octave bandwidths for 5-cm acoustic foam treatment: solid line, external; dashed line, no foam; ○, 50% coverage; +, 90% coverage.

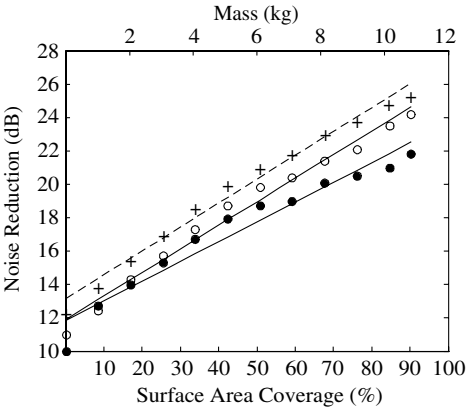

Fig. 20 Noise reduction using 5-cm acoustic foam treatment, with TPS, as a function of area coverage and mass: ●, 500 Hz; ○, 2000 Hz; +, 5000 Hz.

This was significantly higher than what was measured for the fairing with no TPS (7.2, 6.7, and 6.6 dB, respectively). The results in Fig. 18 appear to follow a linear trend as was observed in the no TPS tests. It is apparent that the slopes of the linear regressions were different for the three bandwidths. This indicates that the foam performed better for the 5000 Hz bandwidth than for the 500 Hz bandwidth. At 93% coverage, the reduction over the 500 Hz bandwidth was about 17 dB. It is remarkable that the thin foam treatment was able to damp the low frequency response that well (6 dB above no foam treatment).

Figure 19 shows the external and internal spatially averaged 1/3-octave band levels as a function of frequency for the 5-cm foam tests over the 5000 Hz bandwidth. The external load was computed to be about 94.1 dB (re: 20 μPa). In this case, the foam was able to provide some, albeit little, noise reduction below 100 Hz. The performance of the foam appears constant above 2000 Hz.

Figure 20 summarizes the average measured noise reductions for the 5-cm treatment as a function of surface area and mass for all three bandwidths. The external acoustic loads for these tests were approximately 108 dB (500 Hz), 105 dB (2000 Hz), and 94 dB (5000 Hz). The noise reduction with no foam treatment was approximately 10 dB (500 Hz), 11 dB (2000 Hz), and 12 dB (5000 Hz). The slope of the 2000 Hz data and the 5000 Hz data was very similar. At maximum coverage (93%), the noise reduction was approximately 25.3 dB over the 5000 Hz bandwidth, 1.5 dB more than for the 2.5-cm case. However, the noise reduction for the 500 Hz bandwidth was nearly 22 dB, which is about 5 dB more than the 2.5-cm case. This was expected, because the thicker foam treatment is better able to couple and damp the low frequency acoustic modes.

Figure 21 shows the external and internal spatially averaged 1/3-octave band levels for the 10-cm foam tests. Only two internal measurements are presented—the no foam case and for 42% coverage (test data were only taken to 42% coverage due to schedule

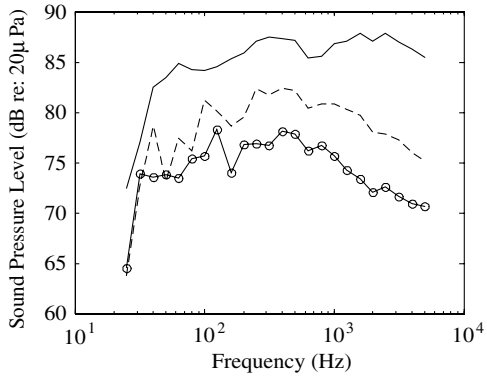

Fig. 21 Spatially averaged sound pressure levels in third octave bandwidths for 10-cm acoustic foam treatment: solid line, external; dashed line, no foam; ○, 42% coverage.

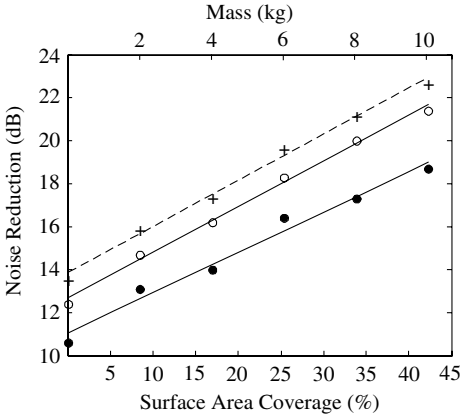

Fig. 22 Noise reduction using 10-cm acoustic foam treatment, with TPS, as a function of area coverage and mass: ●, 500 Hz; ○, 2000 Hz; +, 5000 Hz.

limits). The external disturbance level was computed to be about 99.6 dB. For 42% coverage, the data indicated modest attenuation down to about 40 Hz. Examination of the PSD plots (not shown) revealed that the foam treatment was able to couple with and damp the first, second, and third axial acoustic modes.

Figure 22 summarizes the average measured noise reductions for the 10-cm treatment as a function of surface area and mass for all three bandwidths. The external acoustic loads for these tests were approximately 111 dB (500 Hz), 107 dB (2000 Hz), and 100 dB (5000 Hz). The noise reduction with no foam treatment was measured to be about 10.5 dB (500 Hz), 12 dB (2000 Hz), and 13.9 dB (5000 Hz). At 42% surface area coverage, the noise reduction was about 23 dB (5000 Hz). For comparison, the noise reduction of the 2.5-cm blanket at approximately 42% coverage was 19.5 dB (5000 Hz), and for the 5-cm blanket at 42% coverage was about 20 dB. The noise reduction for the 500 Hz bandwidth at 42% coverage was almost 19 dB.

Having presented a large amount of test data from the individual tests, some figures of merit will be tabulated for comparison and analysis. The averaged noise reductions measured without acoustic foam are summarized in Table 1. For the 5000 Hz bandwidth, the TPS added approximately 7 dB to the noise reduction, which is attributable to mass loading, structural damping, and acoustic absorption. Notice that for the bare fairing, the noise reduction decreased with increasing bandwidth, which resulted from the low amplitude of the nonresonant (i.e., off-resonance) response at low frequency (this is apparent in Fig. 15, where the separation between the external and internal no foam plots is greater at low frequency than at higher frequency). For the TPS-treated fairing, this trend was reversed as a result of the frequency dependent benefits of the TPS (i.e., the TPS provided more acoustic isolation at higher frequency).

Table 2 summarizes the performance of the acoustic foam computed over 5000 Hz. The noise reduction is given for 50 and 93% surface area coverage and for each foam thickness. This table excludes the 5-cm measurements on the bare fairing and compares only the results taken on the TPS-treated fairing. As expected, the thicker acoustic treatment provided more reduction. At 50% coverage, all three treatments exceeded an order of magnitude reduction in the sound pressure level (i.e., 20 dB).

Table 1 Noise reduction of the fairing with and without TPS

Bandwidth	No TPS	With TPS
500 Hz	7.2 ± 0.1 dB	10.6 ± 0.4 dB
2000 Hz	6.7 ± 0.1 dB	12.1 ± 1.1 dB
5000 Hz	6.6 ± 0.1 dB	13.4 ± 1.1 dB

Table 2 Noise reduction measured over the 5000 Hz bandwidth for acoustic foam treatments

Surface area coverage	25 cm	5 cm	10 cm
0%	14.2 dB	12.3 dB	13.6 dB
50%	21.0 dB	21.1 dB	22.7 dB[a]
93%	23.6 dB	25.3 dB	——

[a]42% surface area coverage.

Table 3 Noise reduction as a function of blanket mass

Bandwidth	25 cm	5 cm	10 cm
500 Hz	0.99 dB/kg	0.99 dB/kg	0.79 dB/kg
2000 Hz	1.58 dB/kg	1.19 dB/kg	0.90 dB/kg
5000 Hz	1.78 dB/kg	1.19 dB/kg	0.90 dB/kg

Table 4 Noise reductions as a function of surface area coverage

Bandwidth	25 cm	5 cm	10 cm
500 Hz	0.21 dB/m^2	0.45 dB/m^2	0.71 dB/m^2
2000 Hz	0.34 dB/m^2	0.54 dB/m^2	0.81 dB/m^2
5000 Hz	0.38 dB/m^2	0.54 dB/m^2	0.82 dB/m^2

An analysis of the slopes of the linear regressions given in Figs. 18, 20, and 22 was performed and is summarized in Tables 3 and 4. In Table 3, the slopes of the linear regressions are given in units of noise reduction (in dB) per unit mass of the acoustic treatment. The thinner treatment had the higher reduction per unit mass relative to the other two treatments, which is reasonable since a kilogram of 2.5-cm material covers more surface area than the same amount of 10-cm material. For a given mass limit, the 2.5-cm foam offered the highest noise reduction per unit mass. In fact, the 2.5-cm material offered nearly twice the performance as the 10-cm material over the 5000 Hz bandwidth. However, this advantage is lost if one is only trying to design for the 500 Hz bandwidth.

Table 4 presents the data in units of reduction per unit area of coverage. The data indicate that if the surface area available for treatment is limited, but the mass of the treatment is not, then the 10-cm treatment offers the best noise control solution. This is reasonable considering that 1 m^2 of 10-cm foam is a considerable amount of acoustic treatment. The 10-cm material clearly offered the greatest performance per unit area, regardless of the bandwidth.

V. Conclusion

Acoustic tests were performed on a grid-stiffened, composite, Minotaur payload fairing. These tests investigated the structural-acoustic dynamics of the fairing that contribute to noise transmission. The effect of the flanking paths, thermal protection system, and melamine acoustic foam were presented. Noise reduction measurements were conducted in an acoustic laboratory using an approximately diffuse loading at levels between 90 and 111 dB over three separate test bandwidths. Experimental uncertainty was minimized through repeated testing and averaging.

The test data showed that physical details such as separation rails, gaps, ports, and hatches can be important for correctly predicting noise transmission. Acoustic flanking paths increased noise transmission, with low frequency acoustic resonances being more strongly excited than higher frequency resonances. The internal response of the first three acoustic resonances was nearly an order of magnitude greater than the external level for 1.2% removed surface area.

The thermal protection system provided acoustic absorption of the impinging disturbance load, increased the structural damping, and increased the effective mass of the fairing. Without the thermal protection system, the noise reduction was 6–7 dB, while with the thermal protection system, the noise reduction was about 10–14 dB, depending on the bandwidth.

Melamine foam samples were tested at high sound pressure levels (∼136 dB) and revealed that absorption/reduction was fairly constant with increasing sound pressure levels. This leads us to

conclude that noise reduction measured in the laboratory at 100 dB can reasonably be expected at higher disturbance levels such as those experienced during launch. The noise reduction provided by melamine acoustic foam was studied as a function of disturbance bandwidth, surface area coverage, and mass. Three thicknesses were studied: 2.5, 5, and 10 cm. The noise reduction appeared to follow a linear trend with respect to surface area coverage and mass.

The data indicated that the 2.5-cm material offered the highest reduction per unit mass. In fact, for a given mass limit, the 2.5-cm material offered nearly twice the performance as the 10-cm material over the 5000 Hz bandwidth. It was observed that 3 kg of 2.5-cm material provided about 20 dB of reduction across the 5000 Hz bandwidth. However, if mass is not a critical constraint, then the results showed that the 10-cm material yielded the most noise reduction regardless of the bandwidth. These results were based on measurements taken with the thermal protection system applied and with no flanking paths. This does not include the mass of any bagging material that might be required or of devices/materials used to securely attach the acoustic treatment to the fairing interior.

References

[1] Higgins, J., Fosness, E., Wegner, P., and Buckley, S., "Overview of Next Generation Composite Fairing Development," *Proceedings of SPACE 2002*, edited by B. E. Laubscher, American Society of Civil Engineers (ASCE), Reston, VA, March 2002.

[2] *Delta-IV Payload Planner's Guide*, Sec. 4, Delta Launch Services, The Boeing Company, CA, 1999.

[3] *Commercial Taurus User's Guide*, Release 2.0, Sec. 4.3, Orbital Sciences Corporation, 1996.

[4] Eldred, K. M., *Acoustic Loads Generated by the Propulsion System*, NASA SP-8072, 1971.

[5] McInerny, S. A., "Launch Vehicle Acoustics Part 1: Overall Levels and Spectral Characteristics," *Journal of Aircraft*, Vol. 33, No. 3, 1996, pp. 511–517.

[6] McInerny, S. A., "Launch Vehicle Acoustics Part 2: Statistics of the Time Domain Data," *Journal of Aircraft*, Vol. 33, No. 3, 1996, pp. 518–523.

[7] Bergen, T., Himelblau, H., and Kern, D., "Development of Acoustic Test Criteria for the Cassini Spacecraft," *Journal of the IEST*, Vol. 41, No. 1, 1998, pp. 26–38.

[8] Kendall, R., *Evolved Expendable Launch Vehicle Standard Interface Specification*, Tech. Rept., Aerospace Corporation, Sept. 2000.

[9] *Acoustic Protection on Payload Fairings of Expendable Launch Vehicles*, U.S. Patent 5,670,758, Assigned to Oerlikon-Contraves (AG) and Dornier (GmbH), Sept. 1997.

[10] Gibson, G., Janssen, S., Bradford, L., and Groom, R., "Overview of the Development of Dynamic Environments for Atlas V Launch Vehicles," *Journal of Spacecraft and Rockets*, Vol. 41, No. 5, 2004, pp. 779–786.

[11] *Delta-IV Payload Planner's Guide*, Sec. 3, Delta Launch Services, The Boeing Company, CA, 1999.

[12] Wegner, P., Higgins, J., and Van West, B., "Application of Advanced Grid-Stiffened Structures Technology to the Minotaur Payload Fairing," *AIAA/ASME/ASCE/AHS/ASC Structures, Structural Dynamics and Materials Conference Proceedings*, AIAA, Reston, VA, 2002, Vol. 2, pp. 1061–1067.

[13] Vipperman, J., Li, D., Avdeev, I., and Lane, S., "Investigation of the Sound Transmission into an Advanced Grid Stiffened Structure," *Journal of Vibration and Acoustics*, Vol. 125, No. 3, 2003, pp. 257–266.

[14] Griffin, S., Lane, S., Hansen, C., and Cazzolato, B., "Active Structural Acoustic Control of a Rocket Fairing Using Proof-Mass Actuators," *Journal of Spacecraft and Rockets*, Vol. 38, No. 2, 2001, pp. 219–225.

[15] Fahy, F., *Sound and Structural Vibration*, 1st ed., Fourth printing, Academic Press, San Diego, CA, 1985, pp. 249–255.

[16] Weissman, K., McNelis, M., and Pordan, W., "Implementation of Acoustic Blankets in Energy Analysis-Methods with Application to the Atlas Payload Fairing," *Journal of the IES*, Vol. 37, No. 4, 1994, pp. 32–39.

[17] Do, T., "Vibroacoustic Modeling Study of the Delta II 10-foot Composite Fairing," *Journal of the IEST*, Vol. 42, No. 6, 1999, pp. 26–33.

[18] Li, D., and Vipperman, J., "Noise Control of a Chamber Core Cylinder Using Cylindrical Helmholtz Resonators," *Proceedings of the ASME International Mechanical Engineering Congress*, edited by H. Sardar, ASME Press, New York, 2003, IMECE03-41978.

[19] Bies, D. A., and Hansen, C. H., *Engineering Noise Control, Theory and Practice*, 2nd ed., E&FN Spon, New York, 1996, p. 279.

[20] Matlab—The Language of Technical Computing, The MathWorks, Inc., copyright 1994–2006, www.mathworks.com [retrieved Oct. 2006].

[21] Bies, D. A., Hansen, C. H., *Engineering Noise Control, Theory and Practice*, 2nd ed., E&FN Spon, New York, 1996, p. 35.

L. Peterson
Associate Editor